

29 Mar 2001, 4:00 pm - 6:00 pm

## Dynamic Behavior of Tailings

O. Flores C.

*Instituto de Ingeniería, UNAM, Mexico*

M. P. Romo O.

*Instituto de Ingeniería, UNAM, Mexico*

Follow this and additional works at: <https://scholarsmine.mst.edu/icrageesd>



Part of the [Geotechnical Engineering Commons](#)

---

### Recommended Citation

Flores C., O. and Romo O., M. P., "Dynamic Behavior of Tailings" (2001). *International Conferences on Recent Advances in Geotechnical Earthquake Engineering and Soil Dynamics*. 41.

<https://scholarsmine.mst.edu/icrageesd/04icrageesd/session01/41>

This Article - Conference proceedings is brought to you for free and open access by Scholars' Mine. It has been accepted for inclusion in International Conferences on Recent Advances in Geotechnical Earthquake Engineering and Soil Dynamics by an authorized administrator of Scholars' Mine. This work is protected by U. S. Copyright Law. Unauthorized use including reproduction for redistribution requires the permission of the copyright holder. For more information, please contact [scholarsmine@mst.edu](mailto:scholarsmine@mst.edu).

# DYNAMIC BEHAVIOR OF TAILINGS

**O. Flores C.**

Engineering Institute, UNAM  
Mexico, D.F.

**M. P. Romo O.**

Engineering Institute, UNAM  
Mexico, D.F.

## ABSTRACT

This article presents results of samples tested on a resonant column apparatus. The samples were formed of soil coming from mining residues (tailings), the testing program makes emphasis in the variables that influence the behavior. Finally, the interpretation of the results is made with a knowledge-based procedure and a Masing type model.

## INTRODUCTION

The two principal dynamic properties for dynamic response of soil deposit are the modulus and that effect the damping ratio: The factors that influence more the variation of these parameters in granular materials are: the shear deformation,  $\gamma$ ; the consolidation stress,  $\sigma'$ , the relative compacity,  $C_r$ , and the number of loading cycles,  $N$  (Hardin and Drnevich, 1972). To these, the method to form the sample, the grain size distribution (Hardin and Richart, 1963), and the consolidation time can be added.

## EXPERIMENTAL PROGRAM

Tests were carried out using resonant column equipment capable of inducing shear strains from  $10^{-5}$  to  $10^{-2}\%$ . Thus, shear moduli and damping ratios were obtained for an ample range of shear strains that allow an estimation of the general patterns of the variations of these parameter variations with shear strains.

The materials tested were tailings retrieved from "La Caridad" (in the state of Sonora, Mexico) and "El Baztan" (in the state of Michoacan, Mexico) mines. The grain size distribution is uniform with a  $d_{50}=0.15$  mm. Samples were formed eliminating the fine particles, except in one case where 30% of fines were included to evaluate their effect (see table 1). All specimens were formed by tamping 12 times (following a fixed pattern, Flores 1997) to reach their 8.8 cm height. The tapper diameter was half the 3.6 cm specimen diameter and weights varying between 0.1 and 3 kg were used. Compaction water content ranged from 5 to 16%. The relative compacity,  $C_r$ , of the samples varied from 55 to 88%.

The samples were consolidated following an isotropic stress path. All the tests were carried out with water drainage open (i.e. in drained conditions). The purpose of this was to evaluate sample volume change due to cyclic loading and to try to define the critical strain at which the deformation rate increase notably.

## PRESENTATION AND ANALYSIS OF RESULTS

### Influence of the consolidation stress

Investigations carried out by Silver and Seed (1971), Hardin and Drnevich (1972a) and Tatsuoka, et al (1978) indicate that to the same level of angular deformation,  $\gamma$ , when increasing the consolidation stress,  $\sigma'$ , shear modulus,  $G$ , increases.

The results of this study, in terms of  $G$  and  $\lambda$  (damping ratio) versus  $\gamma$  are presented in fig 1.  $G_{max}$  was assumed to be equal to  $G$  for the lowest value of  $\gamma$ , achieved in each test. It is accepted that  $G_{max}$  values thus defined are affected by the lowest strain volume variation. It is observed that for values of deformation between  $10^{-5}$  and  $10^{-4}\%$ ,  $G$  and  $\lambda$  remain practically constant, and beyond this interval,  $G$  drops and  $\lambda$  increases. A well defined strain threshold that goes from  $7 \times 10^{-4}$  to  $3 \times 10^{-3}$  % shear strains is defined, as the relative compacity increases from 72.5 to 88 %.

It is evident that the shear modulus increases with growing the consolidation pressures, while damping ratios,  $\lambda$ , decrease. The influence in damping is less significant.

### Influence of the relative compacity

Increases in relative compacity in a granular soil lead to stiffer materials. In the interval of deformation of  $10^{-5}$  to  $10^{-3}\%$  this effect is clear. Passing this interval of deformation, all curves

G- $\gamma$  start following a pattern that leads them to approximately the same shear modulus as indicated in fig 2. Same trends are observed for  $G/G_{max}$  and  $\lambda$  versus  $\gamma$  curves.

Table 1 Characteristics of the tests

MATERIAL	CONTENT OF FINE (%)	Cr (%)	$\sigma_c$ (kg/cm <sup>2</sup> )	$\sigma_{cp}$ (kg/cm <sup>2</sup> )	$\sigma'$ (kg/cm <sup>2</sup> )
La Caridad	30	55	1.250	1.000	0.250
			2.750	1.750	1.000
El Baztan	0	64	1.553	0.534	1.019
			2.516	0.534	1.982
La Caridad	0	69	2.000	0.996	1.004
			2.494	1.246	1.248
			2.928	1.252	1.676
			3.250	1.250	2.000
El Baztan	0	71	1.250	0.750	0.500
			1.500	0.750	0.750
			1.750	0.750	1.000
			2.250	1.000	1.250
La Caridad	0	72.5	1.784	1.258	0.526
			2.040	1.239	0.801
			2.249	1.244	1.005
			2.500	1.252	1.248
			3.000	1.254	1.746
El Baztan	0	83.5	0.750	0.250	0.500
			1.000	0.250	0.750
			1.500	0.500	1.000
			2.000	0.500	1.500
El Baztan	0	85.5	0.750	0.500	0.250
			1.241	0.500	0.741
El Baztan	0	88	1.350	0.500	0.850
			1.624	0.500	1.124
El Baztan	0	88	2.500	0.500	2.000

$\sigma_c$ , All around Pressure;  $\sigma_{cp}$ , Backpressure;  $\sigma'$ , Consolidation pressure

The relationships between the effective pressure to which the soil is subjected, the relative compacity and the maximum shear modulus are presented in the fig 3. It is appreciated that when increasing the relative compacity of the soil, the shear modulus grows and the damping decreases.

The practical implication of this behavior is reflected in the use of horizontal filters in tailings dams. This would attenuate the generation of pore pressures, the effective stresses would increase and consequently tailings dams would be safer.

#### Axial deformation and volumetric changes

Volume and axial deformation were monitored during the tests. The results of fig. 4 show that there exists a threshold

deformation,  $\gamma_{cr}$ , that increases with  $Cr$ , and  $\sigma'$ . This critical deformation varies within the same interval as obtained from the shear modulus versus shear strain curves. This result indicates that under dynamic conditions, if the soil is permeable enough to allow water to drain, there exists a critical strain above which the deformation rate increases significantly. Equivalently, for undrained conditions pore water pressure would accumulate faster.

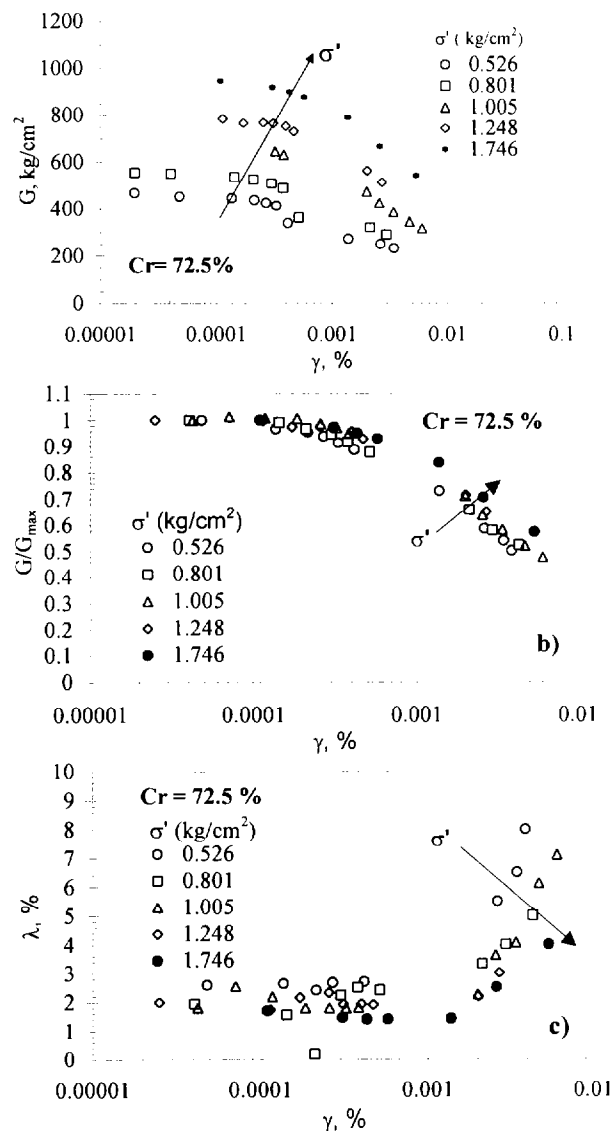


Fig. 1. Influences of the consolidation effort in the dynamic parameters.

#### MODELING OF THE NON LINEAR RELATIONSHIPS G- $\gamma$ AND $\lambda$ - $\gamma$

##### Davidenkov's model

This Masing type of model has been used to reproduce the behavior of Mexico City clays (Romo, 1990; Romo and Ovando, 1995) and granular material (Flores and Romo, 1997).

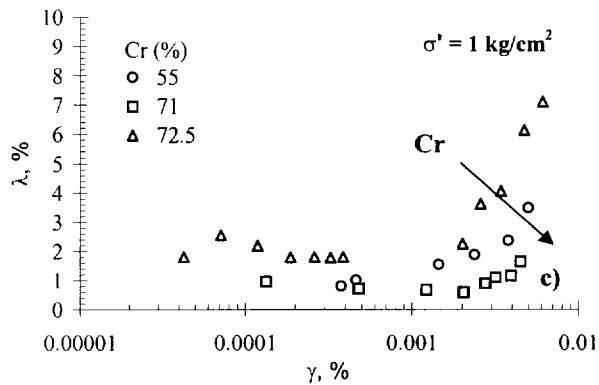
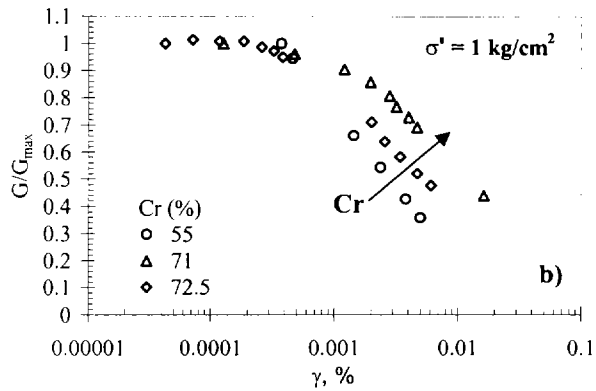
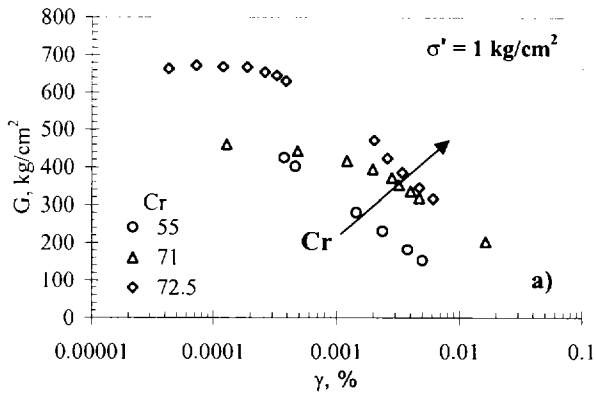


Fig. 2. Influences of the relative compaction in the dynamic parameters.

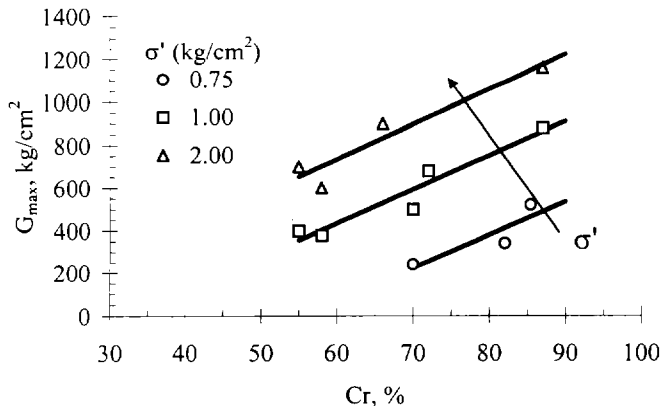


Fig. 3. Relationship of  $G_{max}$  with  $\sigma'$  and  $Cr$ , for  $\gamma=10^{-4}\%$ .

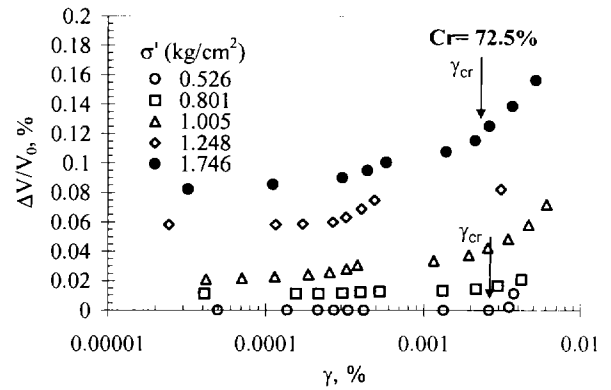
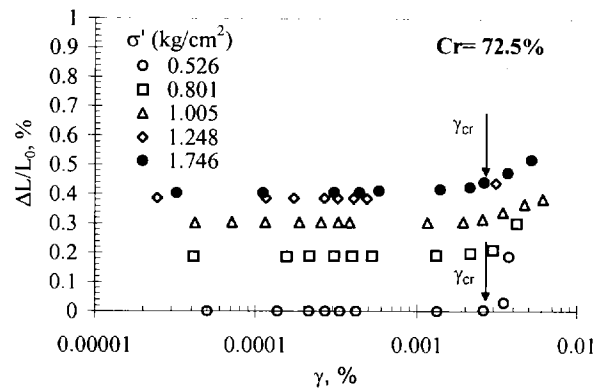


Fig. 4. Lineal deformation and changes of volume.

The equation of the skeleton curve is given by

$$\tau = G\gamma \quad (1)$$

where

$$G = G_{max} [1 - H(\gamma)] \quad (2)$$

The function  $H(\gamma)$  is obtained from the results of dynamic laboratory tests, adjusting an expression to the curve of attenuation  $G/G_{max}$  versus  $\gamma$ , of the type

$$H(\gamma) = \left[ \frac{(\gamma/\gamma_r)^{2B}}{1 + (\gamma/\gamma_r)^{2B}} \right]^A \quad (3)$$

Knowing the function  $H(\gamma)$  and  $G_{max}$ , values of  $G$  for any angular deformation can be defined.  $A$  and  $B$  are soils parameters that define the geometry of the curve  $G-\gamma$ , and  $\gamma_r$  it is the angular deformation corresponding to 50% of modulus degradation.

Hardin and Drnevich (1972) proposed the following relationship between shear modulus and damping ratio

$$\lambda = \lambda_{max} \left( 1 - \frac{G}{G_{max}} \right) \quad (4)$$

From eq (2)

$$\frac{G}{G_{\max}} = [1 - H(\gamma)] \quad (5)$$

Substituting  $\frac{G}{G_{\max}}$  in eq (4), we obtain

$$\lambda = \lambda_{\max} H(\gamma) \quad (6)$$

It seems appropriate to modify eq (6) to account for the maximum  $\lambda_{\max}$  and minimum  $\lambda_{\min}$  values of damping for a particular soil (Romo, 1990). Thus, if  $H(\gamma) \rightarrow 0$ ,  $\lambda = \lambda_{\min}$ , and if  $H(\gamma) \rightarrow 1$ ,  $\lambda = \lambda_{\max}$ . The resulting equation is

$$\lambda = (\lambda_{\max} - \lambda_{\min}) H(\gamma) + \lambda_{\min} \quad (7)$$

Where  $\lambda_{\min}$  is the value of the damping ratio for small angular deformations (i.e.  $10^{-4}\%$ ), and  $\lambda_{\max}$  its value for large deformations (i.e. near dynamic failure).

From the experimental results obtained in this study, values of the soil parameters  $\gamma_r$ , A and B were determined. It was found that A and B were nearly constant and  $\gamma_r$  depended on Cr, as shown in figs 5 and 6.

Considering all the experimental results, a value of  $\lambda_{\min}=2\%$  was defined and a  $\lambda_{\max}=20\%$  was assumed on the bases of damping ratios for fine granular soils.

A comparison between experimental and model-computed shear moduli and damping ratios is included in fig 7. The model reproduces much better the modulus curves than the damping ones.

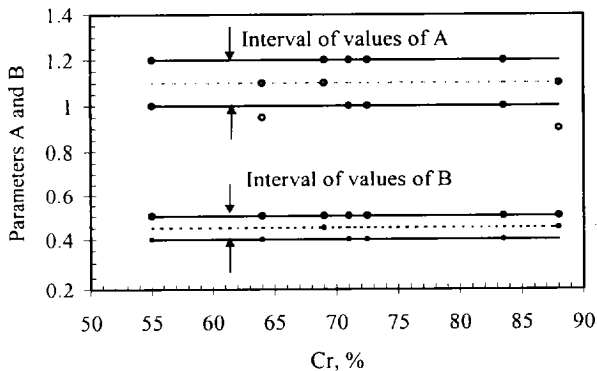


Fig. 5. Variation of the parameters A and B with Cr.

### Neural Networks

Neural Networks can be used for a wide variety of learning tasks. They should be considered as mathematical tools, similar to linear regression analysis. The key feature of neural

networks over regression analysis is that neural networks use non-linear mathematics and therefore can be used to model highly complex and non-linear functions.

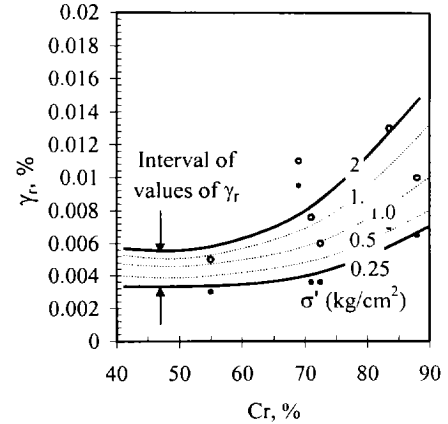


Fig. 6. Relationship between  $\gamma_r$  and Cr.

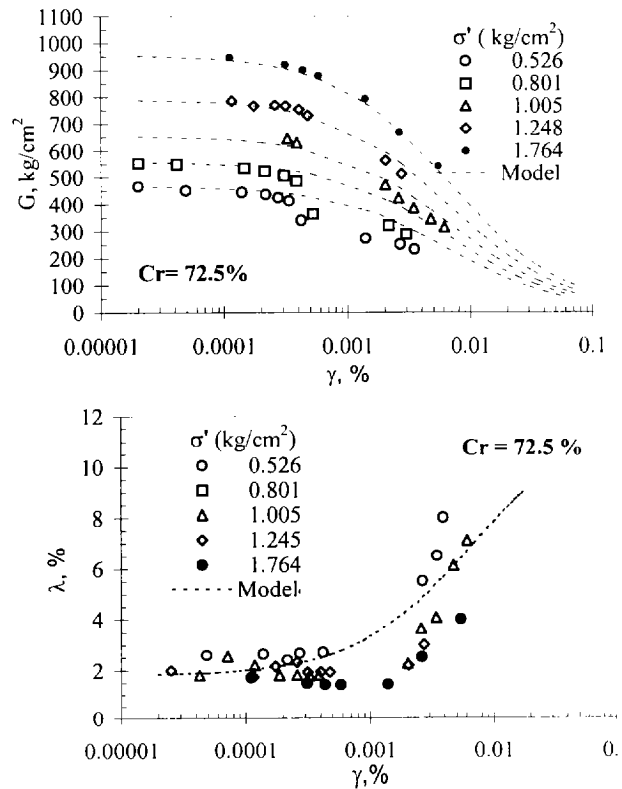


Fig. 7. Comparison of experimental results with the Davidenkov's model.

A learning task consists of a set of data from which training examples are formed. Each training example is usually integrated by input data and the desired network response. Use of a neural network to learn this set of data (training the network) requires the user to make a number of decisions related to the use of the available training methods. Selecting the appropriate method consists of configuring a neural

network and selecting algorithms (learning rules) for training the network. A network accepts an input vector and generates a response in the form of an output vector. This network consists of a set of processing elements (nodes) connected by weights. Choosing a neural network includes selecting network architecture and, then, selecting the kind of processing elements comprising the network. The network architecture determines how the nodes are connected; the number and characteristics of processing elements selected for each layer of the network will affect the overall complexity and performance of the network.

The processing element choice is defined as a combination of a processing element function (input function) and a transfer function. The network output response is adapted by modifying the weights on the connections. Using an error function that measures the distance between the desired output vector and the current actual output vector, a learning algorithm adjusts the weights in the network to reduce the error over the set of training examples.

Multilayer Normal Feed Forward (MNFF) is the most commonly used architecture type, and it is generally recommended for most applications. In this paper only the MNFF is used. The specialized notation for architecture definition used in this study ( $m \times h \times o$ ) is interpreted as follows:  $m$  is the number of input cells,  $h$  is the number of processing units in the hidden layer and  $o$  represents the number of output cells.

The net that was used to predict the shear modulus consists of four layers. Its topology is shown in fig 8. The activation function for the first layer was linear and gaussian for the rest of the layers.

The input variables are the consolidation stress,  $\sigma'$ , the relative compacity of the sample,  $C_r$ , and the angular deformation,  $\gamma$ . The output variable is the shear modulus,  $G$  (Romo et al, 1998).

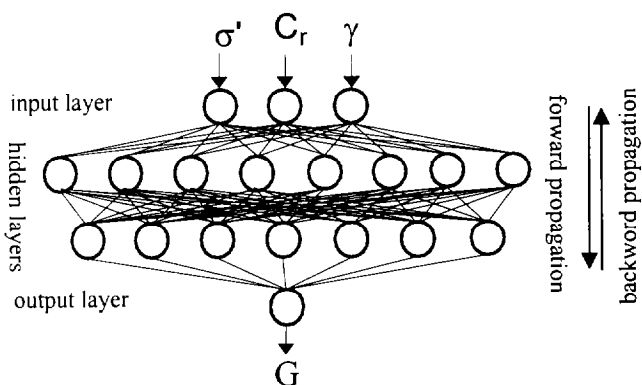


Fig. 8. Architecture of a neural network.

Fig 9 presents the results of four of the tests that were used to verify the predictive capacity of the network. As can be seen, the experimental and network computed values are very near to each other. Stressing the accuracy that can be achieved with this technique. The correlation between experimental and network's value in the training and prediction stages are 0.996 and 0.958, respectively.

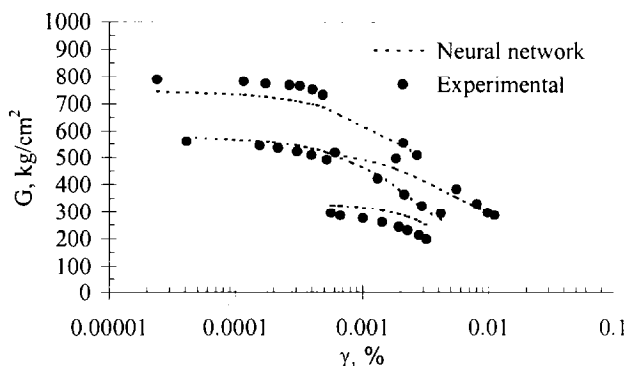


Fig. 9. Comparison between the experimental results and those obtained with the neuronal network.

Comparison between the analytic and network predictions

To verify the predictive capacity of these models, the result of the five tests used for this propose are shown in table 2. To feed the analytic method the parameters A, B,  $\gamma_r$  and  $G_{\max}$  were obtained from figs 3, 5 and 6, while the neural network input data,  $C_r$ ,  $\sigma'$  is given in table 1 and  $\gamma$  was obtained from graphics like there are shown in fig 9.

Table 2 Data to feed the models

Test data		Obtained of the figs 8, 10 and 11			
$C_r$ %	$\sigma'$ $\text{kg/cm}^2$	A	B	$\gamma_r$ %	$G_{\max}$ $\text{kg/cm}^2$
72.5	0.526	1.1	0.45	0.0052	450
	0.801	1.1	0.45	0.0056	585
	1.005	1.1	0.45	0.006	670
	1.248	1.1	0.45	0.0067	775
	1.746	1.1	0.45	0.0079	950

Comparisons are presented in the fig 10. As seen, the model that better approaches the experimental values is the neural network, particularly for shear moduli above  $600 \text{ kg/cm}^2$ .

According to these comparisons it would seem that both models are capable of reproducing the dynamic behavior of tailings materials. Thus, it may be argued that as more information becomes available the analytic model parameters may be generalized and the weights of the network refined, so that the need for extensive laboratory testing would be reduced.

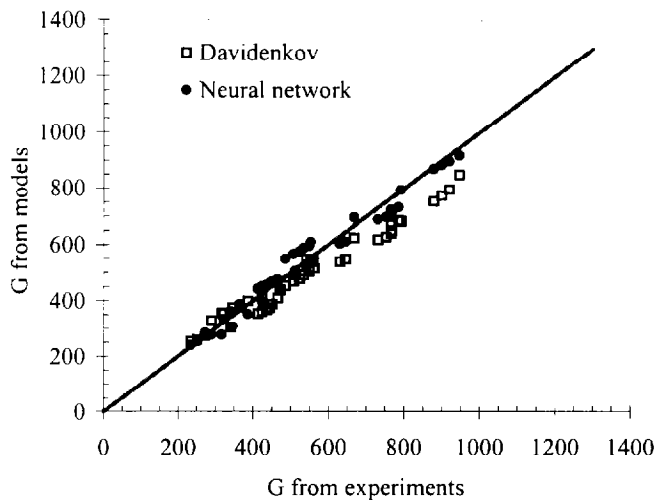


Fig. 10. Correlation between the experimental results and those obtained with both models.

## CONCLUSIONS

The first part of the study consisted on verifying how the relative compacity and the consolidation stress affected the dynamic parameters of the tailing materials. It was observed that when they increased shear moduli increase and damping ratios were reduced. This agrees with the general knowledge accumulated for fine granular material.

From the experimental results it was possible to define a threshold shear deformation. This critical deformation was shown to vary between 0.0007 and 0.003%. Of course this range may be wider for other tailings materials. The predicting capabilities of two models were evaluated. Both procedures yielded satisfactory results with maximum of 12%, in the case of Davidenkov's and 8% for neural networks. The results, however, seem to indicate that the precision of the neural network is considerably higher when the shear modulus of the soil exceeds about 600 kg/cm<sup>2</sup>.

## BIBLIOGRAPHY

- Flores, C. O. [1997]. *Comportamiento dinámico de jales*. M. Sc. thesis, UNAM (in Spanish).
- Flores, C.O. y Romo, M.P. [1997]. *Comportamiento de los jales de la mina El Herrero*. Internal report of the Institute of Engineering, UNAM.
- Hardin, B.O. y Richart, F.E. [1963]. *Elastic wave velocities in granular soils*. Journal of SMF Div., Proc., of ASCE, Vol. 89, pp 33-65.
- Hardin, B.O., Drnevich, V. P. [1972]. *Shear modulus and damping in soils: design equations and curves*. Journal of the Soils Mechanics and Foundation Division, ASCE, Vol. 98, No. SM7, July, pp 667-692.

Hardin, B. O. y Drnevich, V. P. [1972]. *Shear modulus and damping in soils I, measurements and parameters effects*. Journal of SMF Div., Proc., ASCE, Vol. 98, No. SM 6, pp 603-624.

Romo, O.M. y Ovando, S. E. [1995]. *Comportamiento dinámico de las arcillas de la Sonda de Campeche*. Series of the Engineering Institute, UNAM, No. 567, January.

Romo, M.P., [1990]. *Comportamiento dinámico de la arcilla de la ciudad de México y su repercusión en la Ingeniería de Cimentaciones*. Congress: The underground of the Valley of Mexico basin and their relationship with the Engineering of Foundations to five years of the earthquake, SMMS, September, pp 83-94.

Romo, O.M. Rangel, J.L., Flores, C.O., y García, S.R. [1998]. *Aplicaciones de las redes neuronales a la Geotecnia*. National Congress of Soils Mechanics, Puebla, Mexico, November.

Silver, M.L. y Seed, B. [1971]. *Volume changes in sands during cyclic loading*. Journal of the Soil Mechanics and Foundation Division, ASCE, Vol. 97, No. SM9, September, pp 1171-1182.

Tatsuoka, F., Iwasaki, T. y Takagi, Y. [1978]. *Hysteretic damping of sands under cyclic loading and its relation to shear modulus*. Soils and Foundations, Japanese Society of Soil Mechanics and Foundation Engineering, Vol. 18, No. 2. June., pp 26-40.